MOLECULAR AND CELLULAR BIOLOGY, Apr. 1989, p. 1553–1565
0270-7306/89/041553-13$02.00/0

Vol. 9, No. 4

# Posttranslational Regulation of Keratins: Degradation of Mouse and Human Keratins 18 and 8

D. A. KULESH,[1] G. CECEÑA,[1] Y. M. DARMON,[2] M. VASSEUR,[3] AND R. G. OSHIMA[1]*

*Cancer Research Center, La Jolla Cancer Research Foundation, La Jolla, California 92037,[1] and Centre International de Recherches Dermatologiques, Valbonne,[2] and Universite de Paris VII, Paris,[3] France*

Received 30 September 1988/Accepted 4 January 1989

**Human keratin 18 (K18) and keratin 8 (K8) and their mouse homologs, Endo B and Endo A, respectively, are expressed in adult mice primarily in a variety of simple epithelial cell types in which they are normally found in equal amounts within the intermediate filament cytoskeleton. Expression of K18 alone in mouse L cells or NIH 3T3 fibroblasts from either the gene or a cDNA expression vector results in K18 protein which is degraded relatively rapidly without the formation of filaments. A K8 cDNA containing all coding sequences was isolated and expressed in mouse fibroblasts either singly or in combination with K18. Immunoprecipitation of stably transfected L cells revealed that when K8 was expressed alone, it was degraded in a fashion similar to that seen previously for K18. However, expression of K8 in fibroblasts that also expressed K18 resulted in stabilization of both K18 and K8. Immunofluorescent staining revealed typical keratin filament organization in such cells. Thus, expression of a type I and a type II keratin was found to be both necessary and sufficient for formation of keratin filaments within fibroblasts. To determine whether a similar proteolytic system responsible for the degradation of K18 in fibroblasts also exists in simple epithelial cells which normally express a type I and a type II keratin, a mutant, truncated K18 protein missing the carboxy-terminal tail domain and a conserved region of the central, α-helical rod domain was expressed in mouse parietal endodermal cells. This resulted in destabilization of endogenous Endo A and Endo B and inhibition of the formation of typical keratin filament structures. Therefore, cells that normally express keratins contain a proteolytic system similar to that found in experimentally manipulated fibroblasts which degrades keratin proteins not found in their normal polymerized state.**

Intermediate filaments (IF) likely result from the polymerization of tetrameric subunits of individual IF proteins, resulting in relatively insoluble filaments of approximately 10 nm in diameter (21, 55). IF proteins are divided into five types: type I, acidic keratins; type II, neutral-basic keratins; type III, vimentin, desmin, and glial fibrillary acidic protein; type IV, neurofilament (NF) proteins; and type V, lamins (55). Endo B and Endo A, the homologous murine forms of keratin 18 (K18) and keratin 8 (K8), respectively, are type I and type II proteins first detectable at the four- to eight-cell stage, before overt differentiation to trophectoderm (6, 9, 42). The genes encoding Endo A and Endo B (7, 29, 44, 51, 56) and K18 and K8 (31, 32, 43) represent some of the earliest differentially expressed genes yet isolated from mammalian embryos. In adults, expression of these keratin proteins is restricted primarily to a variety of simple epithelial tissues (37), although expression in other cell types does occur (5). The tissue-specific expression of K18 and K8 could be considered intermediate between that of constitutively expressed genes and specialized differentiated functions such as β-globin, α-fetoprotein, or even the epidermal keratins which are expressed in only a few specialized cell types.

In vivo, type III chains (vimentin, desmin, or glial fibrillary acidic protein) usually form homopolymer filaments but are also known to form heteropolymers with the other type III chains (8, 46, 47, 52). The mammalian type IV chains, NF-M and NF-H, generally form heteropolymers with NF-L in vitro, whereas NF-L forms homopolymer IF structures (20, 33, 38). Keratin filaments, however, are obligate heteropolymer IFs, formed in vivo from particular type I and type II subunits which are usually coexpressed as preferential pairs (53, 54, 55a). In vitro, isolated type I and II keratins pair promiscuously, resulting in normal-appearing IFs (26). An intriguing aspect of IF biology is that this apparently coordinate expression of the particular pairs of keratins usually results in equal amounts of type I and type II keratins within cells. This phenomenon is particularly evident for K8 and K18 when they are the only keratins expressed (16, 18, 42, 45).

Despite a wealth of information on the structure of IF proteins, their functions remain largely unclear. The demonstration that the transient expression of a truncated keratin subunit can interfere with the normal polymerization state of keratin filaments within cells (1) suggested that the general strategy of expressing mutant polypeptides to impair the normal function of a protein by competition (27) might be successful in determining the functions of K18 and K8.

We showed previously that after transfection, the K18 gene can be efficiently expressed in murine fibroblasts that do not express the endogenous gene. However, in the absence of a complementary type II keratin partner, the K18 protein is degraded and keratin IFs are not formed (31). In the study reported here, we isolated and expressed a cDNA clone for K8 in mouse fibroblasts that had previously received the K18 gene. This resulted in the formation of stable keratin filaments. Thus, the presence of a type I and a type II keratin appears both necessary and sufficient for keratin filament formation in fibroblasts. Furthermore, we show that overexpression of a truncated K18 protein interferes with normal keratin filament organization in parietal endodermal cells, resulting in accelerated degradation of the keratin proteins.

* Corresponding author.

## MATERIALS AND METHODS

**Isolation and characterization of human K8 cDNA.** Human K8 cDNA was isolated by screening a lambda gt11 cDNA library prepared from placental RNA (35) with an Endo A probe, the α2 pseudogene (56). The cDNA insert was removed by digestion with *Eco*RI and subcloned into pGEM-1 in both orientations to yield plasmids pK811 and pK812. Transcription of the *Bam*HI-digested pK811 plasmid by T7 RNA polymerase and subsequent translation of the RNA in vitro resulted in immunoprecipitable K8 that was indistinguishable from K8 recovered from HeLa or BeWo human cells (data not shown). These results and Northern (RNA) hybridization experiments with radioactive RNA probes derived from pK811 and pK812 indicated that the human K8 cDNA was cloned in the sense orientation relative to the T7 polymerase promoter in pK811 and that the cDNA copy appeared to be full length with respect to its protein-coding capacity. The 5′ end of the human K8 cDNA was sequenced by the method of Sanger et al. (49), modified to use 7-deaza-2-dGTP (3, 36) and deoxyadenosine 5′-[α-$^{35}$S]thiotriphosphate (4), using either sequencing-grade Klenow enzyme (Boehringer Mannheim Biochemicals, Indianapolis, Ind.) or modified T7 DNA polymerase (Sequenase; U.S. Biochemical Corp., Cleveland, Ohio). The double-stranded sequencing was done with both the SP6 and T7 pGEM-1 sequencing primers and six suitable internal 17-mer oligonucleotide primers. The final sequence was assembled from data of 22 different sequencing reactions on both strands, using the GEL program of the BIONET computer system (IntelliGenetics, Mountain View, Calif.).

**Construction of expression vectors.** Human K8 and K18 (43) cDNAs were subcloned into the *Bam*HI and *Hin*dIII sites, respectively, of the pHβAPr-1-gpt human actin promoter expression vector (designated LK442 in this report) (25) by adding appropriate linkers to the *Eco*RI ends of the cDNA fragments (Fig. 1). These constructions, designated LK442-K8 and LK442-K18, respectively, contained an additional selectable transcriptional unit derived from pSV2gpt (39). The cDNA sequences were expected to be transcribed as fusion mRNAs containing the 5′ untranslated first exon and the first intron of the human β-actin gene and used the simian virus 40 (SV40) 3′ termination and polyadenylation signals (Fig. 1). A deletion mutant of the 3′ region of the K18 cDNA was constructed by digestion of LK442-K18 with *Bam*HI and religation. This construction consisted of the LK442 vector and the first 1,070 base pairs of the K18 cDNA, resulting in removal of the last 275 base pairs of the K18 cDNA coding region, the 68-nucleotide (nt) 3′ noncoding region, and the 16-nt poly(A) tail. This construction, LK442-K18-1070 (Fig. 1), coded for the first 340 amino acids of the K18 protein. The mutant protein is referred to as K18-340. The *Eco*RI fragments of both K8 and K18 (43) cDNAs were also cloned into the *Eco*RI site of the pECE expression vector (14), resulting in vectors pECE-K8 and pECE-K18 (Fig. 1). The cDNA sequences were transcribed by the SV40 early promoter and used the SV40 polyadenylation signals. The pECE-K18M vector was generated by excising the K18 cDNA from pECE-K18 by digestion with *Kpn*I and insertion of the fragment into *Kpn*I-digested pECE. This resulted in removal of the K18 polyadenylation signal and the poly(A) tail without loss of any coding sequences.

**Cells and media.** L cells deficient in thymidine kinase (Ltk$^-$), HR9 mouse parietal endodermal cells (10), and NIH 3T3 cells were maintained as previously described (40, 41).

**DNA transfections and selections.** Ltk$^-$ cells that express the transfected K18 gene have been described previously (31). The transfected L-cell clone previously characterized and termed L3 is designated LK18 in this report. LK18 cells were transfected with the LK442-K8 construction and selected for expression of the bacterial guanine phosphoribosyltransferase gene by growth in medium containing 1.6 mM xanthine, 30 μg of mycophenolic acid per ml (39), and 400 μg of G418 per ml. Three clones examined all expressed K8; two of these, expressing the highest levels of K8, were examined in detail. Data for one representative clone, designated LK18+K8, are discussed below. LK8 cells were isolated by transfection of Ltk$^-$ cells with the LK442-K8 vector and selection for guanine phosphoribosyltransferase expression. The three clones examined all expressed K8; the highest expresser, designated LK8, was examined in detail.

NIH 3T3 cells were cotransfected with pECE-K8, pECE-K18, or both plasmids along with plasmid pSV2Neo at a molar ratio of approximately 10:1 (cDNA expression vector to pSV2Neo). Three of four clones derived from the transfection with pECE-K8 expressed K8 protein. Of six clones derived from the transfection of both cDNA expression vectors and pSV2Neo, one expressed K8 and one expressed both K8 and K18. Expression of the K18 cDNA in NIH 3T3 cells was achieved by transfection with a modified pECE-K18 vector that was deleted for both the K18 polyadenylation signal and the poly(A) tail (pECE-K18M). After cotransfection with pSV2Neo, the highest expresser of nine clones was examined further.

**Immunoprecipitation.** Metabolic labeling of cells with [$^{35}$S]methionine (150 μCi/ml), lysate preparation, immunoprecipitation, and gel electrophoresis were performed as previously described (31, 41). Antiserum to Endo A or Endo B was used to precipitate Endo A and K8 or Endo B and K18, respectively (40). All immunoprecipitations were performed in antibody excess. For pulse-chase experiments, equal amounts of radioactive lysate were used for the initial time points. Equal volumes of lysate were then used for subsequent incubation in nonradioactive medium. Film exposures were quantitated by densitometry with an LKB laser densitometer and appropriately exposed films.

**Immunofluorescent labeling.** Immunofluorescent staining was performed on methanol-fixed cells as previously described (28, 40) except that phosphate-buffered saline (pH 7.4) was used instead of 50 mM borate buffer in each washing step. Monoclonal antibody TROMA1 was used for immunofluorescent staining of Endo A and K8 (6), and rabbit antiserum against Endo B (28) was used to detect Endo B, K18, and K18-340. The K8.13 broad-specificity keratin monoclonal antibody (22) was purchased from Sigma Chemical Co. (St. Louis, Mo.).

## RESULTS

**Isolation of human K8 cDNA.** To determine whether IFs could be formed in fibroblasts if both K8 and K18 proteins were present simultaneously, a cDNA clone containing the complete coding sequence for the K8 protein was isolated and subsequently expressed. Previously characterized isolates of human K8 lacked sequences coding for the N terminus of the protein (32). Comparison of DNA sequences of portions of the newly isolated K8 cDNA with the partial sequence previously reported confirmed the identity of the isolate. In vitro translation of RNA transcribed from the isolate followed by immunoprecipitation and sodium dodecyl sulfate-gel analysis and comparison of the in vitro

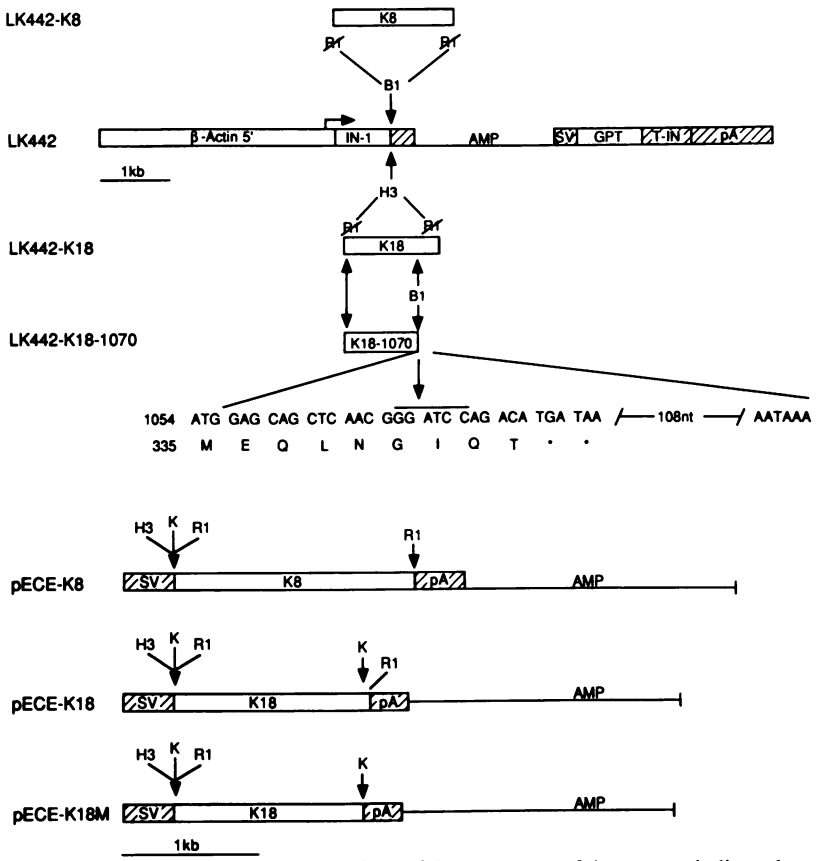


FIG. 1. K8 and K18 expression vectors. Schematic representations of the structures of the vectors indicated on the left are shown. Plasmid sequences are represented by single lines. Direction of transcription of all genes is from left to right. Abbreviations: B1, *Bam*HI; H3, *Hin*dIII; K, *Kpn*I; RI, *Eco*RI, IN-1, human β-actin first intron; SV, SV40 early promoter; gpt, bacterial guanine phosphoribosyltransferase gene; t-IN, SV40 small t-antigen intron; pA, SV40 fragment containing termination and polyadenylation signals; kb, kilobase. The approximate start of transcription of the LK442 series of vectors is indicated by the bent arrow. The K8 and K18 cDNAs were inserted into either the unique *Bam*HI or *Hin*dIII site of the pHβAPr-1-gpt vector (25) (here designated LK442) to generate LK442-K8 and LK442-K18. The truncated cDNA expression vector LK442-K18-1070 was generated from LK442-K18 by digestion with *Bam*HI. All of the inserts are driven by the human β-actin promoter. The 5′ noncoding first exon and the first intron of the actin gene are included but contribute no coding sequences. The inserted cDNA fragments are followed by a fragment of SV40 containing polyadenylation signals. The second transcription unit of these vectors is derived from pSV2gpt and is expected to contain the SV40 early promoter and the bacterial guanine phosphoribosyltransferase gene, followed by the SV40 t-antigen intron and SV40-derived polyadenylation signals. The expanded portion of LK442-K18-1070 shows the nucleotide and amino acid sequences of the 3′ junction as well as the two additional SV40-derived codons added before two translational termination signals. A putative polyadenylation signal, AATAAA, is located 108 nt downstream of the translational termination codon. The K18 and K8 cDNAs were also inserted into the pECE expression vector (14) at the unique *Eco*RI site. pECE-K18M was constructed by removing the K18 cDNA fragment from pECE-K18 by digestion with *Kpn*I and insertion into pECE. The *Kpn*I site in the K18 cDNA cuts within the 3′ noncoding region, thus removing the K18 polyadenylation signal and poly(A) tail.

transcription product with cellular K8 mRNAs by Northern blot analysis indicated that the K8 cDNA was near full length (data not shown). However, comparison of the K8 sequence with that of its mouse homolog indicated that the K8 cDNA may have lacked some of the 5′ noncoding leader, because the Endo A cDNA contained a 170-nt leader whereas that of the K8 cDNA had only 35 nt preceding the ATG initiation codon.

The complete sequence of the K8 cDNA, including the previously unreported 5′ coding sequence, is shown in Fig. 2A. The two underlined portions specify the internal and the 3′-region sequences that were found to be identical with the previously published sequence for K8 (32) except for an additional 6 nt at the extreme 3′ end, immediately preceding the 14-nt poly(A) tail. The full sequence was 1,734 nt long; it had a single open reading frame beginning with the ATG at nt 36 and ended with the termination codon at nt 1485. The nucleotide sequence of the human K8 cDNA was 81% identical with the corresponding region of the mouse Endo A cDNA sequence (50). The deduced amino acid sequence of the open reading frame resulted in a protein of 483 amino acids with a calculated molecular weight of 53,629. At the amino acid level, the two proteins were 87% identical. The protein sequence of the previously unreported head region of K8 is compared with that of Endo A in Fig. 2B. The head region of K8 was six residues shorter than that of its mouse counterpart. In contrast, the head region of K18 was nine residues longer than that of Endo B, its mouse homolog. The remainder of the protein sequences of K8 and Endo A were very similar to those described previously (32, 50).

**Stabilization of K18 by K8 expression in mouse cells.** The K8 cDNA was inserted into two different mammalian expression vectors (Fig. 1), one driven by the human β-actin promoter (LK442-K8) and the second driven by an SV40 promoter (pECE-K8). In addition, the full-length K18 cDNA (43) was inserted into the pECE vector to provide an

A

```
1    GGTTCGGCCC GCCTGCCTCC ACTCCTGCCT CCACCATG

39   TCC ATC AGG GTG ACC CAG AAG TCC TAC AAG GTG TCC ACC TCT GGC CCC CGG GCC TTC AGC AGC CGC TCC TAC ACG AGT GGG CCC GGT TCC
     Ser Ile Arg Val Thr Gln Lys Ser Tyr Lys Val Ser Thr Ser Gly Pro Arg Ala Phe Ser Ser Arg Ser Tyr Thr Ser Gly Pro Gly Ser

129  CGC ATC AGC TCC TCG AGC TTC TCC CGA GTG GGC AGC AGC AAC TTT CGC GGT GGC CTG GGC GGC GGC TAT GGT GGG GCC AGC GGC ATG GGA
     Arg Ile Ser Ser Ser Ser Phe Ser Arg Val Gly Ser Ser Asn Phe Arg Gly Gly Leu Gly Gly Gly Tyr Gly Gly Ala Ser Gly Met Gly

219  GGC ATC ACC GCA GTT ACG GTC AAC CAG AGC CTG CTG AGC CCC CTT GTC CTG GAG GTG GAC CCC AAC ATC CAG GCC GTG CGC ACC CAG GAG
     Gly Ile Thr Ala Val Thr Val Asn Gln Ser Leu Leu Ser Pro Leu Val Leu Glu Val Asp Pro Asn Ile Gln Ala Val Arg Thr Gln Glu

301  AAG GAG CAG ATC AAG ACC CTC AAC AAC AAG TTT GCC TCC TTC ATA GAC AAG GTA CGG TTC CTG GAG CAG CAG AAC AAG ATG CTG GAG ACC
     Lys Glu Gln Ile Lys Thr Leu Asn Asn Lys Phe Ala Ser Phe Ile Asp Lys Val Arg Phe Leu Glu Gln Gln Asn Lys Met Leu Glu Thr

399  AAG TGG AGC CTC CTG CAG CAG CAG AAG ACG GCT CGA AGC AAC ATG GAC AAC ATG TTC GAG AGC TAC ATC AAC AAC CTT AGG CGG CAG CTG
     Lys Trp Ser Leu Leu Gln Gln Gln Lys Thr Ala Arg Ser Asn Met Asp Asn Met Phe Glu Ser Tyr Ile Asn Asn Leu Arg Arg Gln Leu

489  GAG ACT CTG GGC CAG GAG AAG CTG AAG CTG GAG GCG GAG CTT GGC AAC ATG CAG GGG CTG GTG GAG GAC TTC AAG AAC AAG TAT GAG GAT
     Glu Thr Leu Gly Gln Glu Lys Leu Lys Leu Glu Ala Glu Leu Gly Asn Met Gln Gly Leu Val Glu Asp Phe Lys Asn Lys Tyr Glu Asp

579  GAG ATC AAT AAG CGT ACA GAG ATG GAG AAC GAA TTT GTC CTC ATC AAG AAG GAT GTG GAT GAA GCT TAC ATG AAC AAG GTA GAG CTG GAG
     Glu Ile Asn Lys Arg Thr Glu Met Glu Asn Glu Phe Val Leu Ile Lys Lys Asp Val Asp Glu Ala Tyr Met Asn Lys Val Glu Leu Glu

669  TCT CGC CTG GAA GGG CTG ACC GAC GAG ATC AAC TTC CTC AGG CAG CTG TAT GAA GAG GAG ATC CGG GAG CTG CAG TCC CAG ATC TCG GAC
     Ser Arg Leu Glu Gly Leu Thr Asp Glu Ile Asn Phe Leu Arg Gln Leu Tyr Glu Glu Glu Ile Arg Glu Leu Gln Ser Gln Ile Ser Asp

759  ACA TCT GTG GTG CTG TCC ATG GAC AAC AGC CGC TCC CTG GAC ATG GAC AGC ATC ATT GCT GAG GTC AAG GCA CAG TAC GAG GAT ATT GCC
     Thr Ser Val Val Leu Ser Met Asp Asn Ser Arg Ser Leu Asp Met Asp Ser Ile Ile Ala Glu Val Lys Ala Gln Tyr Glu Asp Ile Ala

849  AAC CGC AGC CGG GCT GAG GCT GAG AGC ATG TAC CAG ATC AAG TAT GAG GAG CTG CAG AGC CTG GCT GGG AAG CAC GGG GAT GAC CTG CGG
     Asn Arg Ser Arg Ala Glu Ala Glu Ser Met Tyr Gln Ile Lys Tyr Glu Glu Leu Gln Ser Leu Ala Gly Lys His Gly Asp Asp Leu Arg

939  CGC ACA AAG ACT GAG ATC TCA GAG ATG AAC CGG AAC ATC AGC CGG CTC CAG GCT GAG ATT GAG GGC CTC AAA GGC CAG AGG GCT TCC CTG
     Arg Thr Lys Thr Glu Ile Ser Glu Met Asn Arg Asn Ile Ser Arg Leu Gln Ala Glu Ile Glu Gly Leu Lys Gly Gln Arg Ala Ser Leu

1029 GAG GCC GCC ATT GCA GAT GCC GAG CAG CGT GGA GAG CTG GCC ATT AAG GAT GCC AAC GCC AAG TTG TCC GAG CTG GAG GCC GCC CTG CAG
     Glu Ala Ala Ile Ala Asp Ala Glu Gln Arg Gly Glu Leu Ala Ile Lys Asp Ala Asn Ala Lys Leu Ser Glu Leu Glu Ala Ala Leu Gln

1119 CGG GCC AAG CAG GAC ATG GCG CGG CAG CTG CGT GAG TAC CAG GAG CTG ATG AAC GTC AAG CTG GCC CTG GAC ATC GAG ATC GCC ACC TAC
     Arg Ala Lys Gln Asp Met Ala Arg Gln Leu Arg Glu Tyr Gln Glu Leu Met Asn Val Lys Leu Ala Leu Asp Ile Glu Ile Ala Thr Tyr

1209 AGG AAG CTG CTG GAG GGC GAG GAG AGC CGG CTG GAG TCT GGG ATG CAG AAC ATG AGT ATT CAT ACG AAG ACC ACC GGC GGC TAT GCG GGT
     Arg Lys Leu Leu Glu Gly Glu Glu Ser Arg Leu Glu Ser Gly Met Gln Asn Met Ser Ile His Thr Lys Thr Thr Gly Gly Tyr Ala Gly

1299 GGT TTG AGC TCG GCC TAT GGG GAC CTC ACA GAC CCC GGC CTC AGC TAC AGC CTG GGC TCC AGC TTT GGC TCT GGC GCG GGC TCC AGC TCC
     Gly Leu Ser Ser Ala Tyr Gly Asp Leu Thr Asp Pro Gly Leu Ser Tyr Ser Leu Gly Ser Ser Phe Gly Ser Gly Ala Gly Ser Ser Ser

1389 TTC AGC CGC ACC AGC TCC TCC AGG GCC GTG GTT GTG AAG AAG ATC GAG ACA CGT GAT GGG AAG CTG GTG TCT GAG TCC TCT GAC GTC CTG
     Phe Ser Arg Thr Ser Ser Ser Arg Ala Val Val Val Lys Lys Ile Glu Thr Arg Asp Gly Lys Leu Val Ser Glu Ser Ser Asp Val Leu

1479 CCC AAG TGA ACAGCTGCGG CAGCCCCTCC CAGCCTACCC CTCCTGCGCT GCCCCAGAGC CTGGGAAGGA GGCCGCTATG CAGGGTAGCA CTGGGAACAG GAGACCCACC
     Pro Lys ***

1588 TGAGGCTCAG CCCTAGCCCT CAGCCCACCT GGGGAGTTTA CTACCTGGGG ACCCCCCTTG CCCATGCCTC CAGCTACAAA ACAATTCAAT TGCTTTTTTT TTTTGGTCCA

1698 AAATAAAACC TCAGCTAGCT CTGCCAAAAA AAAAAAAAA
```

B

```
HEAD
                  10        20        30        40            50        60        70        80        90
KER 8    MSIRVTQKSYKVSTSGPRAFSSRSYTSGPGSRISSSSFSRVG--SSNFRG--GLGGGYG--GASGMGGITAVTVNQSLLSPLVLEVDPNIQAVRTQ
         :::::::::::: :::::::::::::.::::: ::::::::::::  :: :::  : : : :  :. : :::::::::::::::::: ::::::::::::::
ENDO A   MSIRVTQKSYKMSTSGPRAFSSRSFTSGPGARISSSSFSRVGSSSSSFRGSMGTGVGLGGFGGAGVGGITAVTVNQSLLSPLKLEVDPNIQAVRTQ
                  10        20        30        40        50        60        70        80        90
```

FIG. 2. (A) DNA sequence of the human K8 cDNA and the deduced amino acid sequence. Nucleotides 1 to 730 were determined from clones pK811 and pK812. An overlap of 83 nt within the coding region (underlined bases from 647 to 730) with the previously published sequence of the 3′ end of human K8 cDNA (32) was identified, and the two were merged into one continuous K8 sequence. Underlined nucleotides within the 3′ noncoding region were also determined to be identical with the previously published fragment except for six additional bases in our clone immediately preceding the poly(A) tail. The predicted amino acid sequence is shown beneath the DNA sequence. The termination codon (TGA) is indicated (***). The 483 amino acids of the human K8 protein result from a coding region of 1,446 nt along with 39 nt of 5′ and 234 nt of 3′ noncoding sequences. (B) Comparison of the head regions of the human K8 and Endo A proteins. Both amino acid sequences start with the initiation methionine and end with the last amino acid before coil 1A. A perfect amino acid match is represented by a colon; conservative substitution is indicated by a period.

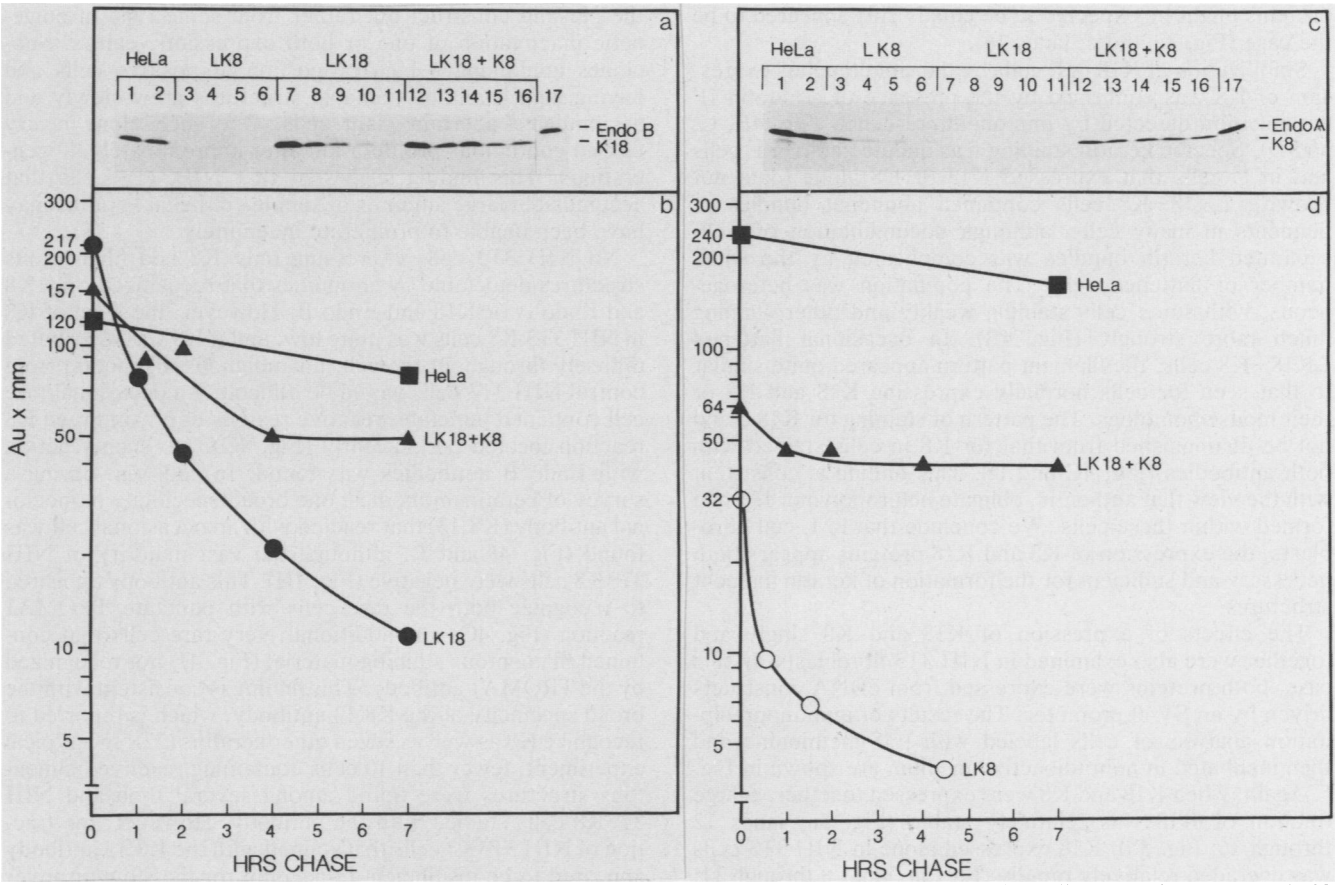


FIG. 3. Expression and turnover of human K18 and K8 in stably transfected mouse L cells. HeLa and L cells expressing the LK442-K8 vector (LK8), the K18 gene (LK18), or both (LK18+K8) were incubated in methionine-free medium supplemented with 150 μCi of [$^{35}$S]methionine per ml and 10% fetal bovine serum for 45 min, washed, and then incubated for the indicated times in nonradioactive complete medium. The lysates were immunoprecipitated with Endo B antiserum, which cross-reacted with the K18 protein (a). Duplicate portions of the lysates were immunoprecipitated with Endo A antiserum, which also recognized the K8 protein (c). In each case, the volume of lysate representing the first time point contained $5 \times 10^6$ cpm of incorporated radioactivity. The same volume of lysate was then used for each subsequent time point. Fluorographic exposures of sodium dodecyl sulfate-gels used to resolve the proteins are shown in panels a and c. HeLa cells that expressed both K18 (a, lanes 1 and 2) and K8 (c, lanes 1 and 2) and HR9 mouse parietal endodermal cells that expressed Endo B (a, lane 17) and Endo A (c, lane 17) were positive controls. Incubation times in nonradioactive medium for LK8 were 0, 0.5, 1.5, and 4.5 h for lanes 3 through 6, respectively; incubation times for both LK18 (lanes 7 through 11) and LK18+K8 (lanes 12 through 16) were 0, 1, 2, 4, and 7 h. Exposure time was 4 days. Positions of Endo B, K18, Endo A, and K8 are indicated on the right. Values of densitometric scans of the appropriate areas of an exposed film are shown in panels b and d in arbitrary units (A multiplied by distance in millimeters).

alternative method for expression of K18. A stably transfected L-cell line that had previously received the K18 gene and been shown to express the K18 mRNA and protein (31) and control L cells were transfected with the LK442-K8 vector. The two clones that expressed K18 and the highest levels of K8 protein and one control that contained only the K8 expression vector were examined in detail for protein expression and stability of the keratin subunits by a pulse-chase experiment, followed by immunoprecipitation and gel analysis (Fig. 3).

K8 and K18 are quite stable in cells that normally express them (13, 31), as confirmed by the results for HeLa cells (Fig. 3a and 3c, lanes 1 and 2; Fig. 3b and 3d). However, L cells that expressed the K18 gene (LK18) turned over newly synthesized K18 protein relatively rapidly (Fig. 3a, lanes 7 through 11; Fig. 3b) (31). K8 expressed alone in L cells was found to be degraded in a similar fashion (Fig. 3c, lanes 3 through 6; Fig. 3d). Thus, both K18 and K8 were unstable in L cells when expressed singly. However, expression of K8 in L cells that had previously received and expressed the K18 gene (LK18+K8) had a dramatic effect on the stability of both K18 and K8. Most of the K8 expressed in LK18+K8 cells was stable, although a minor fraction was degraded within the first hour of the chase period (Fig. 3c, lanes 12 through 16; Fig. 3d). In addition, a significant fraction of the K18 in these cells was similarly resistant to degradation (Fig. 3a, lanes 12 through 16; Fig. 3b). The amount of K18 in these cells after a 7-h incubation in nonradioactive medium appeared to correlate with the level of K8 expression in both clones examined in detail (data for only the higher-expressing clone are shown in Fig. 3). The clone with the higher level of K8 contained a larger fraction of stable K18 during the chase period. The fraction of K18 degraded within the first few hours of the chase period presumably represented the K18 that was in excess of the partner K8. In all clones expressing either one or both human keratins (LK18, LK8, and LK18+K8), induction of homologous mouse forms of the proteins was not detected (Fig. 3a, lanes 3 through 7; Fig. 3c, lanes 8 through 10). If the levels of K18 and K8 found after the longest chase period depend only on the polymerization of K18 and K8, the final levels of the two

proteins might be expected to be equal. This appeared to be the case (Fig. 3a and c, lanes 16).

Stabilization of K18 in L cells by the simultaneous expression of K8 was confirmed by the presence of a keratin IF organization detected by immunofluorescence (Fig. 4B, C, and D). Specific keratin staining was undetectable in L cells and in L cells that expressed K18 or K8 alone (data not shown). LK18+K8 cells contained abundant bundles of filaments in many cells, although documentation of well-separated keratin bundles was complicated by the small number of flattened cells. The population was heterogeneous, with some cells staining weakly and other staining much more strongly (Fig. 4B). In occasional flattened LK18+K8 cells, the filament pattern appeared quite similar to that seen for cells normally expressing K18 and K8 or their mouse homologs. The pattern of staining for K18 could not be distinguished from that for K8 in cells stained with both antibodies (Fig. 4C and D). This finding is consistent with the view that authentic, obligate heteropolymer IFs had formed within these cells. We conclude that in L-cell fibroblasts, the expression of K8 and K18 proteins appears both necessary and sufficient for the formation of keratin filament structures.

The effects of expression of K18 and K8 singly and together were also examined in NIH 3T3 fibroblasts. In this case, both proteins were expressed from cDNA constructs driven by an SV40 promoter. The results of immunoprecipitation analysis of cells labeled with [$^{35}$S]methionine and then incubated in nonradioactive medium are shown in Fig. 5. Again, when K18 and K8 were expressed together, a large fraction of K18 was relatively stable (Fig. 5a, lanes 12 through 16; Fig. 5b). K18 expressed alone in NIH 3T3 cells was degraded relatively rapidly (Fig. 5a, lanes 8 through 11; Fig. 5b). When K8 was expressed together with K18 in NIH 3T3 cells, K8 turned over relatively slowly. However, in contrast to K8 alone in L cells and K18 alone in NIH 3T3 cells, K8 appeared relatively stable in NIH 3T3 cells when expressed alone (Fig. 5c, lanes 3 through 7; Fig. 5d).

The reason why solitary K8 was not degraded quickly in NIH 3T3 cells is unclear because such cells neither expressed the endogenous, complementary mouse Endo B (Fig. 5a, lanes 3 through 7) nor contained immunofluorescence-detectable keratin filaments at a frequency that could account for such stability (see below). Nevertheless, it is apparent that K18 was degraded when expressed alone in NIH 3T3 cells and was stabilized only when K8 was also present, as shown for LK18+K8 cells. Again, no synthesis of a complementary, endogenous keratin was detected in NIH 3T3 cells expressing only K8 (Fig. 5a, lanes 3 through 7) or K18 (Fig. 5c, lanes 8 through 11). In additional experiments, the Endo A gene (56) was expressed in NIH 3T3 cells after transfection, but again no induction of Endo B or other type I keratins was detected (data not shown).

Immunofluorescent staining of the stably transfected NIH 3T3 cells detected keratin filament patterns in cells receiving both the K8 and K18 expression vectors (Fig. 4A, E, and F). Double staining with antibodies recognizing both K18 and K8 showed superimposable patterns (Fig. 4E and F), which suggested that the two proteins were colocalized. Approximately 25% of the cells of the primary clonal isolate, which was transfected with both cDNAs, stained positive for K18-K8 filaments. After subcloning, the proportion of cells staining positive for filaments ranged from approximately 1 to 90% in different clones. Curiously, every subclone contained some positive cells, which suggested that the lack of expression in some transfected cells resulted not from loss of the plasmid construct but rather from some type of epigenetic inactivation of one or both expression vectors. Subclones containing a high proportion of positive cells and having high levels of stainable structures grew slowly and accumulated aberrant giant cells. One such clone nearly ceased continuous proliferation after approximately 40 generations. This finding suggested that NIH 3T3 cells that accumulated large amounts of simple epithelial keratins may have been unable to proliferate indefinitely.

No NIH 3T3 cells expressing only K8 had filamentous structures detectable by antibodies that recognized only K8 and Endo A or K18 and Endo B. However, the level of K8 in NIH 3T3 K8 cells was quite low, and if K8 was distributed diffusely throughout the cell, unambiguous distinction from control NIH 3T3 cells would be difficult. An occasional rare cell contained punctate, reactive regions of presumptive K8 reaction located perinuclearly (Fig. 4G). No such reaction with Endo B antibodies was found. In addition, during a survey of keratin antibodies, one broad-specificity monoclonal antibody (K8.13) that reacted with an occasional cell was found (Fig. 4I and J), although the vast majority of NIH 3T3K8 cells were negative (Fig. 4H). This antibody appeared to recognize both the rare cells with punctate TROMA1 reaction (Fig. 4G) and additional, very rare cells that contained filamentous staining material (Fig. 4J) not recognized by the TROMA1 antibody. This finding is consistent with the broad specificity of the K8.13 antibody, which is reported to recognize K8 as well as seven other keratins (22). In a typical experiment, fewer than 10 cells containing reactive filamentous structures were found among several thousand NIH 3T3K8 cells stained with the antibody. However, the fraction of NIH 3T3K8 cells that stained with the K8.13 antibody appeared to be insufficient to account for the slow turnover of K8 in NIH 3T3 cells. The reactive cells of this recent clonal population may have resulted from the inappropriate expression of an epidermal type I keratin, as has been reported by others (23). Expression of K8 in many or most of the cells of this clone may facilitate detection of the activation of a type I keratin gene by permitting stable keratin filaments to form.

**Disruption of Endo A and Endo B filaments by a truncated K18 protein.** The demonstration that K18, and in some cases K8, is degraded in fibroblasts that lack a partner protein suggests that degradation of keratin proteins that are in excess of a complementary subunit might contribute to the observation that K18 and K8 are commonly found in equal amounts within permissive cells. To determine whether a similar degradation system exists in cells that normally express simple epithelial keratins, we attempted to stably disrupt the polymerization state of Endo A and Endo B in mouse parietal endodermal cells by coexpression of a truncated K18 protein. Our construct (designated LK442-K18-1070 in Fig. 1) retains 1,070 nt of the K18 cDNA and would be expected to code for a protein containing the first 340 amino acids of the K18 protein along with an additional 2 amino acids. This truncated protein (designated K18-340) would not contain the last 50 amino acids of coil 2 (including the conserved sequence TYRRLLEGE found at the end of coil 2 in all IFs) or the 39-amino-acid tail region. The expected molecular weight of K18-340 is 38,057. Transfection of LK442-K18-1070 into HR9 parietal endodermal cells and selection for the linked guanine phosphorsbosyltransferase transcription unit resulted in multiple clones. Of the first six to be examined, four expressed the expected truncated protein; the two with the highest K18-340 expression were examined in detail. Use of polyclonal rabbit antibodies

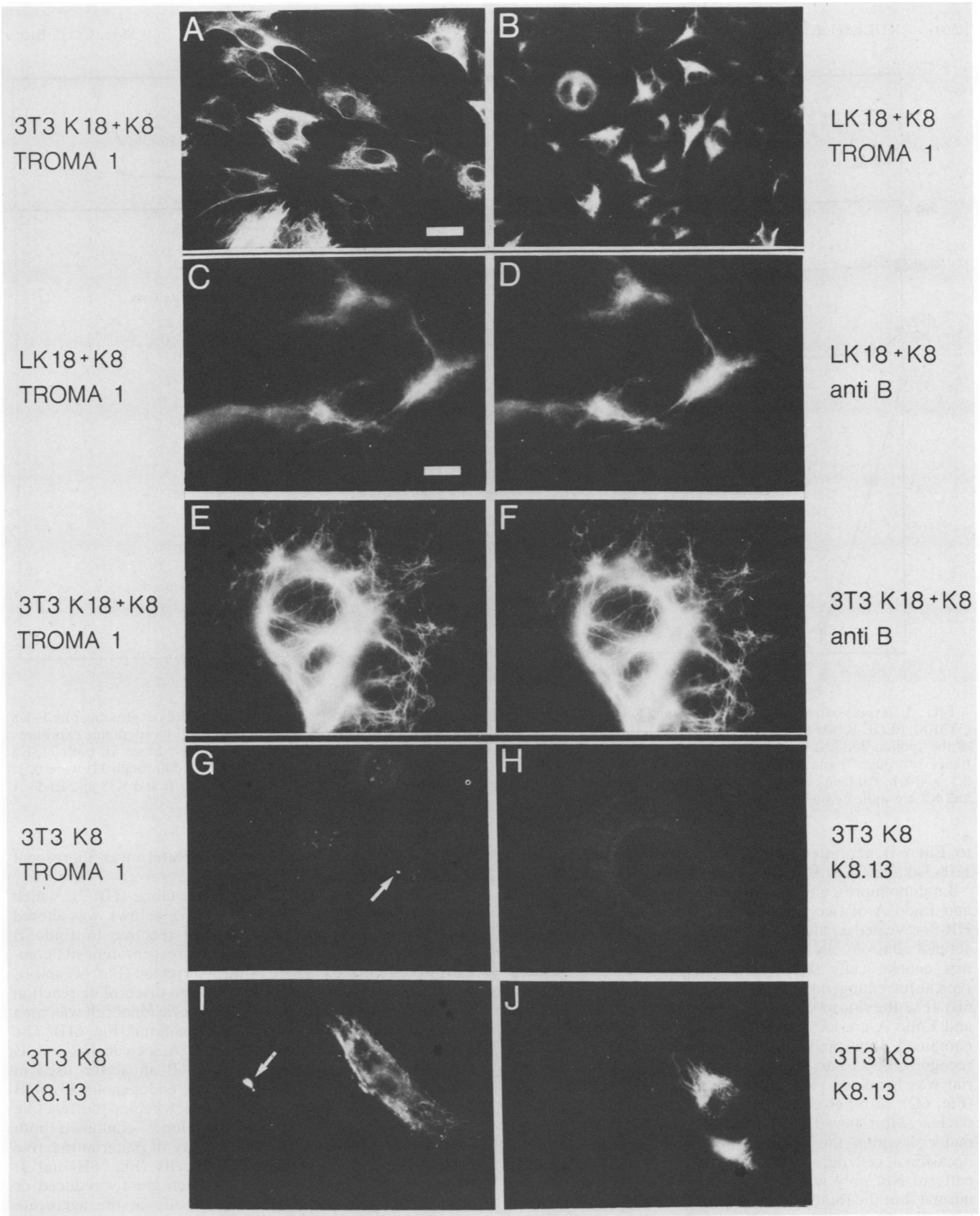


FIG. 4. Immunofluorescent staining of keratin filaments in NIH 3T3 cells and L cells expressing both K18 and K8. (A, E, and F) 3T3K18+K8 cells; (B, C, and D) LK18+K8 cells; (G through J) 3T3K8 cells. Cells were exposed to monoclonal antibody TROMA1, which recognized K8 (A, B, and G), or were double labeled with both TROMA1 and Endo B antibodies that recognized K18 (C and D; E and F) and appropriate rhodamine- or fluorescein-labeled secondary antibodies. Panels H through J were reacted with the K8.13 broad-specificity monoclonal antibody reported to recognize K1, -5, -6, -7, -8, -10, -11, and -18. The strongly fluorescent 3T3K8 cells shown in panels I and J are examples found very rarely (less than once per 1,000 cells). Arrows in panels G and I point to perinuclear aggregate material recognized by TROMA1 and K8.13 in occasional cells. The bar in panel A, which applies also to panels B, G, I, and J, represents 21.7 μm; the bar in panel C, which applies to the remaining panels as well, represents 8.7 μm.

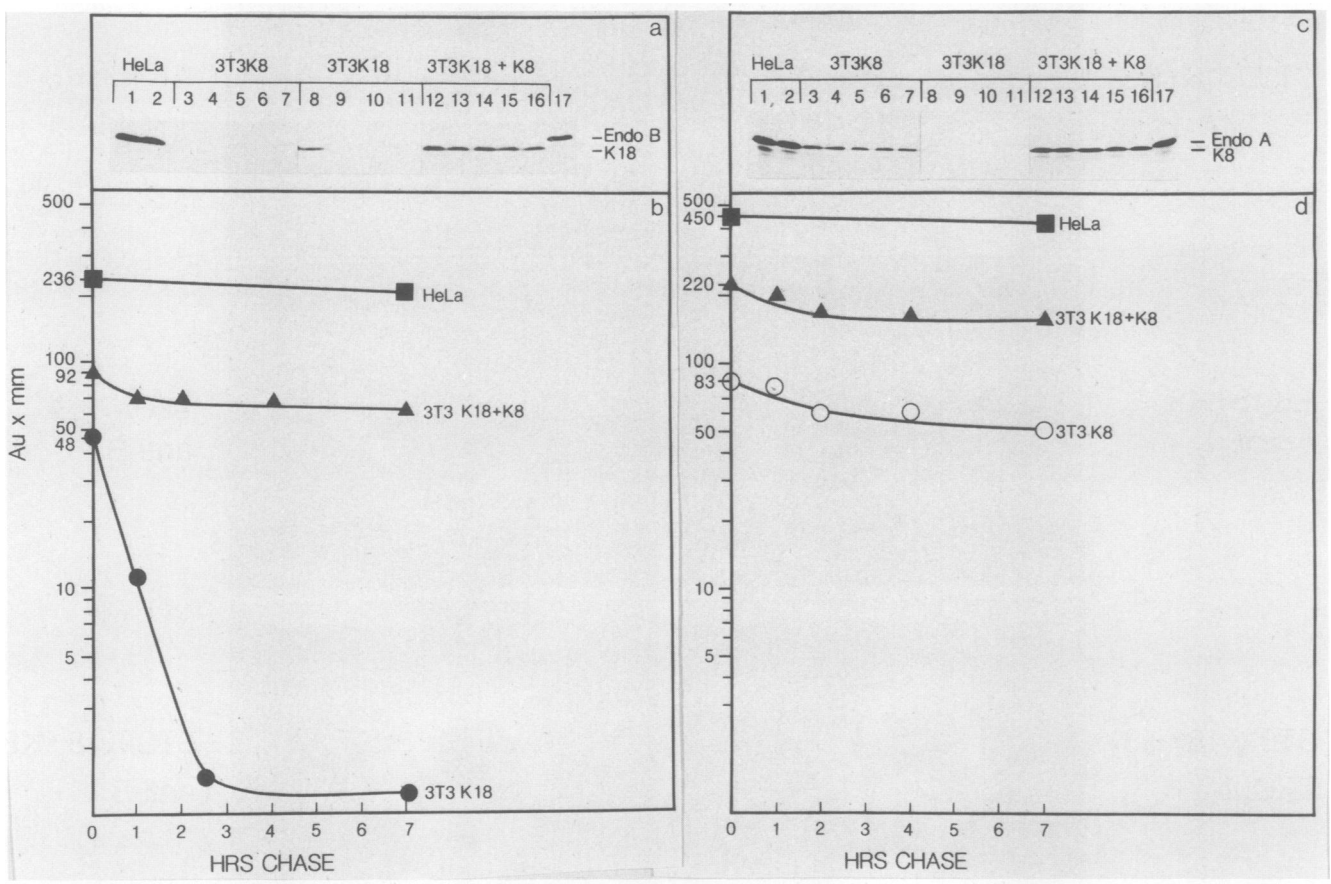


FIG. 5. Expression and turnover of K18 and K8 in stably transfected mouse NIH 3T3 cells. HeLa and NIH 3T3 cells expressing pECE-K8 (3T3K8), pECE-K18M (3T3K18), or both (3T3K18+K8) were analyzed as described in the legend to Fig. 3. (a and c) Fluorographic exposures of the sodium dodecyl sulfate-acrylamide gel used to resolve immunoprecipitated K18 and K8, respectively. Chase times for both 3T3K8 (lanes 3 through 7) and 3T3K18+K8 (lanes 12 through 16) were 0, 1, 2, 4, and 7 h; chase times for 3T3K18 (lanes 8 through 11) were 0, 1, 2.5, and 8 h. All lanes were exposed for 2 days. (b and d) Results plotted as in Fig. 3. Migration positions of Endo B and K18 and Endo A and K8 are indicated on the right.

to Endo B permitted the simultaneous detection of both K18-340 and Endo B.

Immunofluorescent staining with antibodies to Endo B and Endo A of two clones expressing K18-340 (HR-1 and HR-7) revealed a pattern very different from that of similarly stained control cells (Fig. 6). Mouse HR9 parietal endodermal control cells (HR-C) exhibited the staining pattern typical for endogenous Endo B (Fig. 6A) and Endo A (Fig. 6B) IFs. Previous studies have demonstrated that Endo B and Endo A are localized in the same IFs (28). HR-1 cells contained only small localized concentrations of material recognized by Endo B antibodies. In some cells, this material was localized exclusively at the perimeter of the cell (Fig. 6C); in other cells, the fluorescent material was perinuclear. More than 95% of the cells contained no filamentous material within the cytoplasmic regions, even though an occasional cell did exhibit an apparently normal staining pattern. Not only was the pattern of staining altered from normal, but the total amount of accumulated material within the cells was much lower, as judged by the time of photographic exposure necessary for documentation. The staining pattern of Endo A within these cells was similarly altered (Fig. 6D and F). Punctate staining material was found within the cells, often in the perinuclear region or in accumulated material at the outer edge of the cell. The Endo A pattern differed from the Endo B pattern in an additional overall diffuse staining, whereas the Endo B pattern was fluorescent only in the aggregate material.

The staining pattern of the second clone (HR-7), which expressed a higher level of K18-340 (see below), was altered to an even greater extent. Material reactive to Endo B antibodies was found as punctate fluorescent deposits commonly concentrated in the perinuclear region (Fig. 6G and I). Although most of the HR-7 cells had no discernible reaction with Endo A antibodies (Fig. 6J), an occasional cell was seen to contain small deposits of reactive material (Fig. 6H). The diffuse cytoplasmic staining of Endo A seen in HR-1 cells was not evident. Because the Endo B antiserum used in these experiments reacted with both endogenous Endo B and the K18-340 protein, it is unclear whether the reactive material in the two experimental clones contained both keratin proteins. However, the paucity of material reactive with Endo A antibodies in HR-7 cells (Fig. 6H and J) suggested that Endo A may have been greatly reduced or unavailable to the monoclonal antibody in the aggregate material stained by Endo B antibodies. It is clear that the polymerization states of Endo B and Endo A were drastically affected by the expression of K18-340. Both the HR-1 and HR-7 cells proliferated comparably to or slightly faster than the parental line. Taken together, these results indicate that the K18-340 protein efficiently inhibited the normal formation of the Endo A-Endo B IF network in HR9 cells

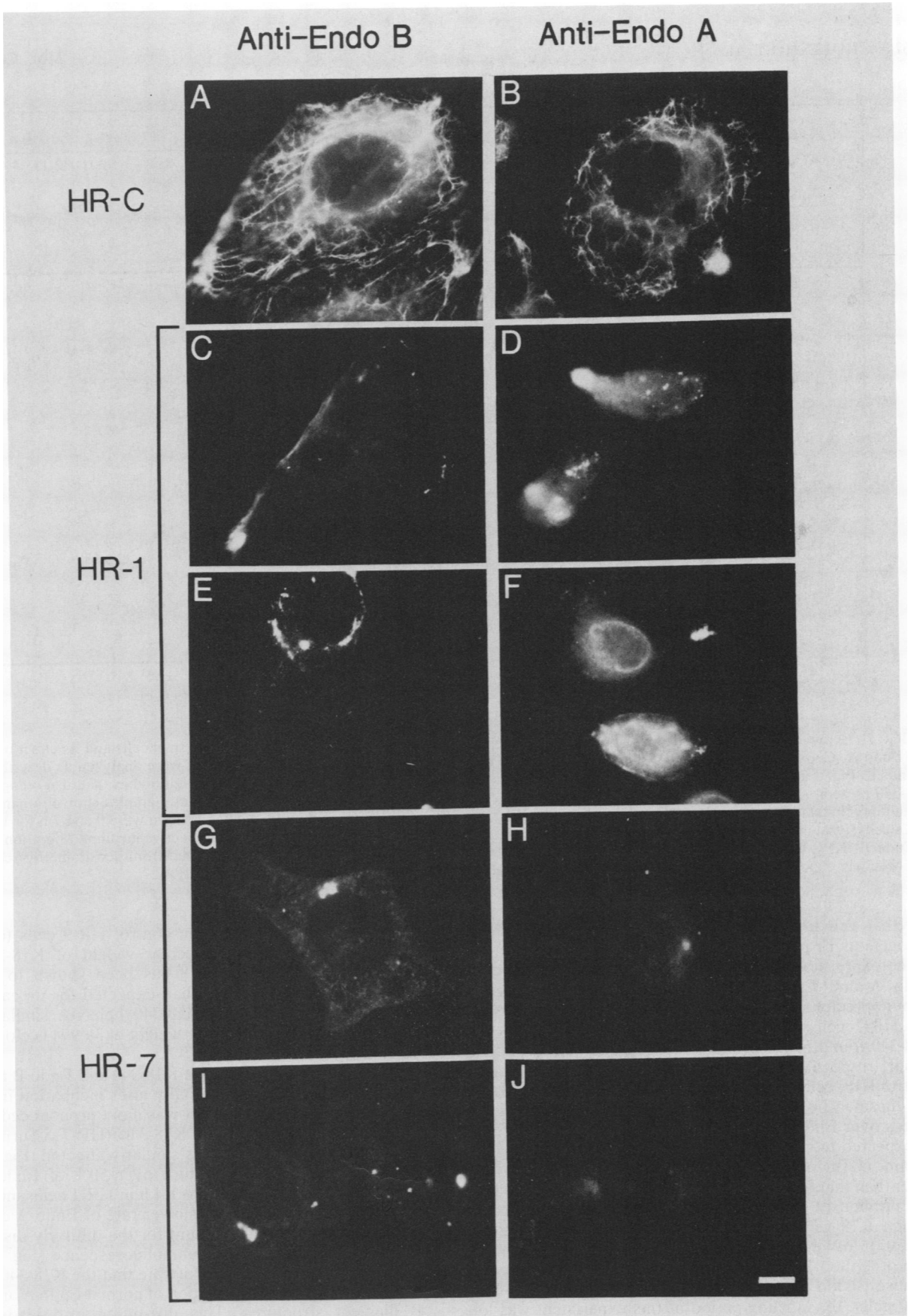


FIG. 6. Immunofluorescent staining of the endogenous keratin filament network of mouse HR9 parietal endodermal cells expressing a truncated K18 protein. (A and B) Control HR9 cells (HR-C); (C through J) two representative HR9 clones (HR-1 and HR-7) that expressed the K18-340 protein stained with the indicated antibodies as described in the legend to Fig. 4. (A, C, E, G, and I) Reactions of Endo B antibodies that also recognized K18 and K18-340; (B, D, F, H, and J) reactions with monoclonal antibody TROMA1. The bar in panel J, which applies to all panels, represents 7.85 μm. Note the punctate antibody reaction in panels G, I, D, and H and the lack of reaction in panel J. Perinuclear reaction is particularly evident in panels E and F, and accumulation of antigen at the periphery of cells is evident in panels C and D.

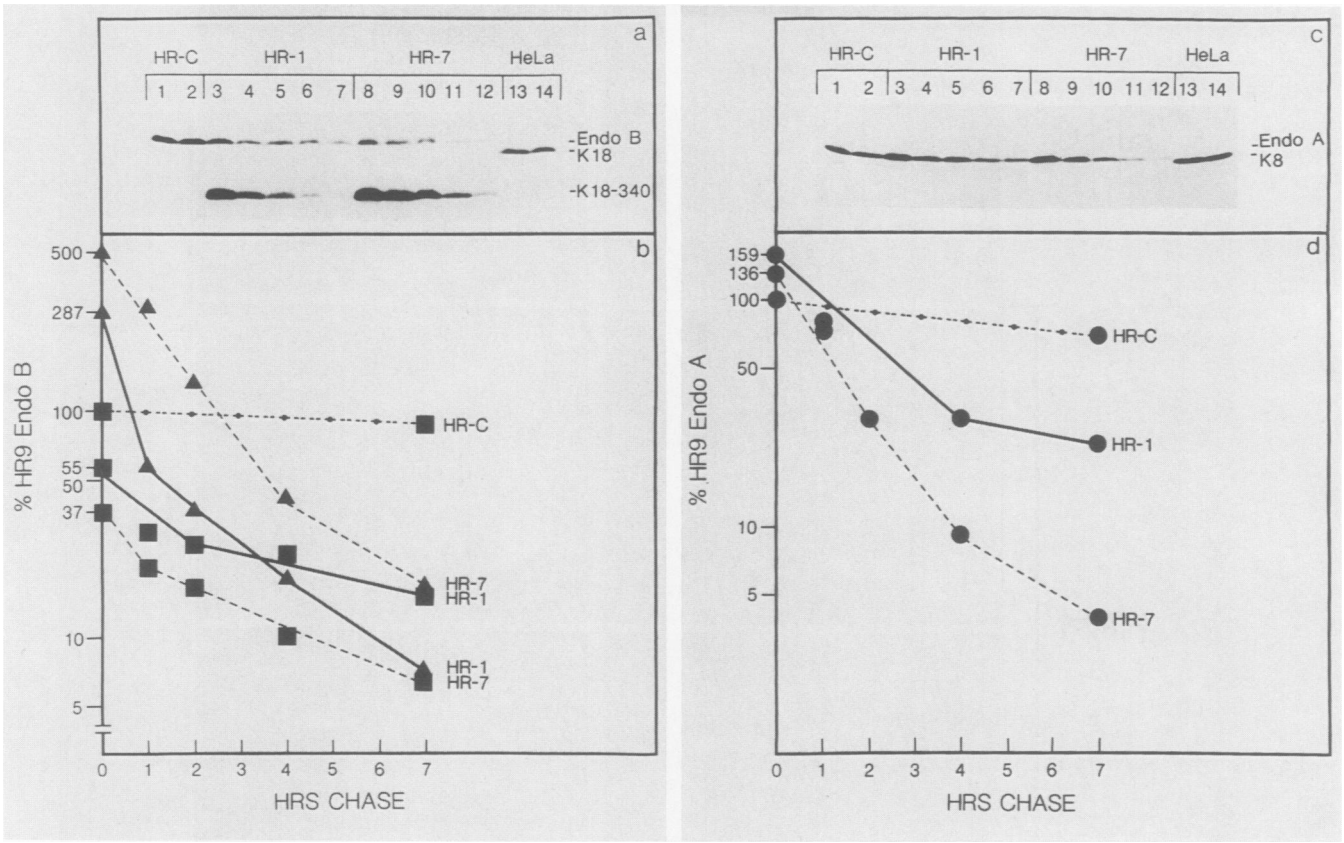


FIG. 7. Expression and turnover of a truncated K18 protein (K18-340) in HR9 mouse parietal endodermal cells and its effect on Endo B and Endo A. Control HR9 cells (HR-C) and HeLa and HR9 cells expressing K18-340 (HR-1 and HR-7) were analyzed as described in the legends to Fig. 3 and 5. Samples shown in panel a were the result of immunoprecipitation with Endo B antibodies that also recognized the K18-340 protein, sodium dodecyl sulfate-gel analysis, and a 2-day fluorographic exposure of the dried gel. Samples shown in panel c were immunoprecipitated with Endo A antiserum in the same way. The incubation times in nonradioactive medium were 0 and 7 h for HR-C and HeLa cells; lysates were prepared from HR-1 and HR-7 cells 0, 1, 2, 4, and 7 h after incubation in nonradioactive medium. Migration positions of Endo B, K18, K18-340, Endo A, and K8 are indicated on the right in panels a and c. Values obtained from densitometric scanning of appropriately exposed films are shown in panels b and d after normalization to the first time point for HR-C.

and that cell lines which continuously exhibit an altered endogenous IF pattern can be established.

The expression of K18-340 and its effect on endogenous Endo A and Endo B protein stability was assessed by immunoprecipitation analysis of metabolically labeled HR-1 and HR-7 cells (Fig. 7). After a 45-min labeling period, K18-340 found in HR-1 and HR-7 cells was 2.9- and 5-fold higher, respectively, than the amount of Endo B found in control HR9 cells (HR-C) (Fig. 7a, lanes 1, 3, and 8; Fig. 7b, 0-h chase). The K18-340 protein was clearly expressed in excess over Endo B in HR-1 and HR-7 cells and thus might be expected to compete efficiently for Endo A binding. The amount of Endo B found in HR-1 and HR-7 cells was also lower than that found in control cells. This result is similar to that previously observed for HR9 cells that expressed the foreign K18 gene (31) and appears to imply some down-regulation of endogenous Endo B synthesis by overexpression of either K18 or, in this case, K18-340. However, because Endo B turned over relatively rapidly in HR-1 and HR-7 cells, the labeling period of this experiment was long enough to permit significant keratin degradation to occur during the incubation in radioactive medium, resulting in an underestimation of the rate of Endo B protein synthesis. Additional experiments indicated that as the labeling period was made shorter, the apparent rate of Endo B synthesis approached the value for the control HR-9 cells (data not shown). The apparent molecular weight of K18-340 was estimated to be 33,851. K18 has been shown to migrate approximately 18% slower than expected for its calculated molecular weight (43). If K18-340 behaves similarly, the corrected apparent molecular weight of 39,994 is close to the calculated value of 38,057.

The amounts of radioactive K18-340 and Endo B from the transfected cells dropped rapidly after incubation in nonradioactive medium. This effect was more pronounced in cells expressing higher levels of K18-340 (HR-7). Turnover of Endo A in the same cells was similarly affected (Fig. 7c and d). The time necessary to turn over 50% of Endo A decreased from more than 7 h to 1.4 h in HR-1 cells and to less than 1 h in HR-7 cells. The slower rate of Endo A degradation in HR-1 cells may account for the diffusely distributed Endo A pattern seen by immunofluorescence (Fig. 6D and F). These experiments demonstrate that the K18-340 human protein can inhibit the formation of normal Endo A and Endo B filament structures. This disruption also leads to an increased degradation of Endo A and Endo B. Thus, a similar proteolytic system that degrades singly expressed K18 and K8 in murine fibroblasts may also exist in cells that normally express the endogenous mouse homologs of K18 and K8.

## DISCUSSION

Whereas K18 and its mouse homolog, Endo B, are normally restricted in expression in adult animals to simple epithelial tissues (37), transfection of the isolated K18 gene into fibroblasts resulted in the expression of both K18 mRNA and K18 protein (31) without induction of the endogenous homologous keratin genes. In addition, this expression appeared quite efficient, since LK18 cells contained only one to two copies of the K18 gene (data not shown). These results, combined with those for K18 and Endo B expression in somatic cell hybrids and chromatin and methylation studies of Endo B, suggest that expression of K18 is not restricted in fibroblasts because of the absence of necessary transcription factors or by the action of *trans*-acting negative regulators (44). Rather, K18 expression may be restricted by an epigenetic inactivation mechanism. The results presented here provide evidence of an additional posttranslational aspect to the regulation of the expression of K18. When K18 is expressed alone in mouse fibroblasts, it is rapidly degraded. The isolation and expression of a K8 cDNA containing all coding sequences permitted us to demonstrate that coexpression of K18 and K8 subunits was necessary and sufficient to stabilize K18, culminating in keratin filament formation within cells. The accumulation of K18-K8 filaments in NIH 3T3 cells resulted in both the generation of aberrant cells and a slower proliferation rate in the highest-expressing clones. This result implies that although the expression of two complementary keratins is sufficient for filament formation, other mechanisms may be necessary for regulating the keratin filament polymerization state to permit orderly cell division. The overexpression of keratin filaments may be biologically relevant to certain cell processes such as the generation of trophoblast giant cells, which accumulate many copies of genomic DNA without cell division while expressing simple epithelial keratins at high levels (2).

Neither expression of K8 in mouse L or NIH 3T3 cells nor expression of Endo A in NIH 3T3 cells resulted in the induction of endogenous Endo B. Thus, the induction of a type I keratin by the expression of a type II keratin in fibroblasts as reported by other investigators (23) appears not to be a general mechanism for all keratins.

Expression of the K8 cDNA showed that K8 was subject to proteolytic degradation in L cells when expressed singly. In NIH 3T3 cells, however, K8 was more stable. This differential stability of K8 appears not to be due to the induction of a complementary mouse type I keratin, as judged by both immunoprecipitation and immunofluorescent staining methods. The detection of K8 in the form of nonfilamentous deposits within some NIH 3T3K8 cells raised the possibility that K8 was in a precipitated form, perhaps unavailable to degradation in NIH 3T3 cells. However, additional analysis of the nonionic detergent-soluble and -insoluble fractions of NIH 3T3K8 and LK8 cells revealed that K8 could be detected in both fractions but that the proportion of K8 recovered in the two fractions was the same in both cell types (data not shown). Therefore, K8 appeared to be in a similar physical state in the two cell types. The difference in the rates of K8 degradation in NIH 3T3 and L cells may reflect a difference in the activity of one or more proteolytic systems in the two cell types. Both K8 and K18 have candidate PEST signal sequences, which are postulated to be responsible for the degradation of various intracellular proteins (48). However, these sequences are located in the head and tail domains of K8 and near the center of K18. Some PEST proteins may be shielded from proteolytic degradation by complexing with a second protein (24). The interaction of K8 and K18 or the interaction of higher-order intermediates of IF formation may similarly safeguard these keratins from degradation.

We did detect very rare NIH 3T3K8 cells that contained keratin filament structures. Although these cells did not react with monoclonal antibody TROMA1, it is possible that this antibody does not recognize a hypothetical hybrid keratin filament composed of K8 and an endogenous, inappropriately expressed type I keratin. The inappropriate expression of such a type I keratin in NIH 3T3 cells has been reported (23). However, the fraction of cells containing such filaments in NIH 3T3K8 cells was extremely low and appeared to be insufficient to account for the stability of K8. Expression of the keratins detected by the K8.13 antibody may be related to the proposed epigenetic suppression of at least certain keratin genes. The inappropriate expression of a previously suppressed type I gene would be facilitated by the forced expression of a complementary type II keratin. The frequency of cells accumulating keratin reactive with the K8.13 monoclonal antibody may reflect the degree to which suppressive mechanisms can maintain type I keratin genes in the inactive state. In this regard, the cell lines expressing only K8 or K18 may be useful as recipients of additional vectors expressing complementary proteins and as test lines for measuring the frequency at which complementary keratin genes are activated either spontaneously or as a result of drug treatment (11).

Inhibition of the filament pattern of Endo A and Endo B in mouse parietal endodermal cells by overexpression of K18-340 is consistent with the results of investigators who have demonstrated that the transient expression of mutant K14 proteins missing the highly conserved, terminal portion of the coil 2 domain dramatically disrupts endogenous keratin networks (1). The molecular level at which K18-340 inhibits Endo A and Endo B filament organization is not yet clear. Magin et al. (34) have shown that similar deletions of the *Xenopus* K8 molecule will nonetheless permit binding to K18 in vitro. Thus, K18-340 might be expected to bind to Endo A, the mouse homolog of K8, thereby directly competing with endogenous Endo B. Whether such hybrid molecules could form stable tetramer intermediates of two type I and two type II keratin subunits or even higher-order structures such as protofilaments remains to be determined. Also, the nature of the residual antigenic material found by immunofluorescent staining of HR-1 and HR-7 cells remains to be investigated at the electron microscope level. These spheroid and irregular antigenic structures appear similar to transient IF protein aggregates found normally in some cell types (19) and in certain pathological states (12, 17).

Our results showing that acidic and basic keratins are stabilized when expressed together suggest that tight coordinate regulation of the mRNA levels of the two keratin proteins may not be necessary to ensure the equal amounts of the proteins commonly found in the cytoskeletons of epithelial cells. Clearly, mechanisms that permit the transcription of the two genes in appropriate cell types are still required. The establishment of both long-term cell lines and possibly transgenic mice with disrupted filament patterns provides intriguing alternatives to the method of antibody injection (15, 30) for the study of the biological function(s) of simple epithelial keratins both in vivo and during development.

## ACKNOWLEDGMENTS

We thank A. Semat for technical assistance and E. Ellis and L. Kedes for making available the pECE and LK442 expression vectors, respectively.

Part of this work was accomplished while R.G.O. was visiting the University of Paris VII. Support from the University of Paris VII and help from D. Paulin in arranging the visit are gratefully acknowledged. This work was supported by Public Health Service grants CA 42302 and CA 33946 to R.G.O. and Cancer Center support grant P30 CA 30199, all from the National Cancer Institute. D.A.K. was supported by Public Health Service postdoctoral training grant T32 CA09497 from the National Cancer Institute. The BIONET computer facility is supported by Public Health Service grant U41 RR 01685 from the National Institutes of Health.

## ADDENDUM IN PROOF

Subsequent to the review of this manuscript, a study describing the expression of Endo B and *Xenopus laevis* K8 in 3T3 cells was published (L. Domenjoud, J. L. Jorcano, B. Breuer, and A. Alonso, Exp. Cell Res. **179**:352–361, 1988). The results presented here are in agreement with their conclusions that both type I and type II keratins are required for filament formation in 3T3 cells and that singly expressed K18 is unstable.

## LITERATURE CITED

1. **Albers, K., and E. Fuchs.** 1987. The expression of mutant epidermal keratin cDNAs transfected in simple epithelial and squamous cell carcinoma lines. J. Cell Biol. **105**:791–806.
2. **Ansell, J. D.** 1975. The differentiation and development of mouse trophoblast, p. 133–144. *In* M. Balls and A. E. Wild (ed.), The early development of mammals. Cambridge University Press, New York.
3. **Barr, P. J., R. M. Thayer, P. Laybourn, R. C. Najarian, F. Seela, and D. R. Tolan.** 1986. 7-Deaza-2'-deoxyguanosine-5'-triphosphate: enhanced resolution in M13 sequencing. BioTechniques **4**:428–432.
4. **Biggin, M. D., T. J. Gibson, and G. F. Hong.** 1983. Buffer gradient gels and $^{35}S$ label as an aid to rapid sequence determination. Proc. Natl. Acad. Sci. USA **80**:3963–3965.
5. **Bosch, F. X., R. E. Leube, T. Achtstatter, R. Moll, and W. W. Franke.** 1988. Expression of simple epithelial type cytokeratins in stratified epithelia as detected by immunolocation and hybridization in situ. J. Cell Biol. **106**:1635–1648.
6. **Brulet, P., C. Babinet, R. Kemler, and F. Jacob.** 1980. Monoclonal antibodies against trophectoderm-specific markers during mouse blastocyst formation. Proc. Natl. Acad. Sci. USA **77**: 4113–4117.
7. **Brulet, P., P. Duprey, M. Vasseur, M. Kaghad, D. Morello, P. Blanchet, C. Babinet, and H. Condamine.** 1985. Molecular analysis of the first differentiations in the mouse embryo. Cold Spring Harbor Symp. Quant. Biol. **1**:51–57.
8. **Cabral, F., M. M. Gottesman, S. B. Zimmerman, and P. M. Steinert.** 1981. Intermediate filaments from Chinese hamster ovary cells contain a single protein. J. Biol. Chem. **256**:1428–1431.
9. **Chisholm, J. C., and E. Houlistom.** 1987. Cytokeratin filament assembly in the preimplantation mouse embryo. Development **101**:565–582.
10. **Chung, A. E., L. E. Estes, H. Shinozuka, J. Braginski, C. Lorz, and C. A. Chung.** 1977. Morphological and biochemical observations on cells derived from the in vitro differentiation of the embryonal carcinoma cell line PCC4-F. Cancer Res. **37**:2072–2081.
11. **Darmon, M., J. F. Nicolas, and D. Lamblin.** 1984. 5-Azacytidine is able to induce the conversion of teratocarcinoma-derived mesenchymal cells into epithelial cells. EMBO J. **3**:961–967.
12. **Denk, H., W. W. Franke, R. Eckerstorfer, E. Schmid, and D. Kerjaschki.** 1979. Formation and involution of Mallory bodies ("alcoholic hyalin") in murine and human liver revealed by immunofluorescence microscopy with antibodies to prekeratin. Proc. Natl. Acad. Sci. USA **76**:4112–4116.
13. **Denk, H., E. Lackinger, K. Zatloukal, and W. W. Franke.** 1987. Turnover of cytokeratin polypeptides in mouse hepatocytes. Exp. Cell Res. **173**:137–143.
14. **Ellis, L., E. Clauser, D. O. Morgan, M. Edery, R. A. Roth, and W. J. Rutter.** 1986. Replacement of insulin receptor tyrosine residues 1162 and 1163 compromises insulin-stimulated kinase activity and uptake of 2-deoxyglucose. Cell **45**:721–732.
15. **Emerson, J. A.** 1988. Disruption of the cytokeratin filament network in the preimplantation mouse embryo. Development **104**:219–234.
16. **Franke, W. W., H. Denk, R. Kalt, and E. Schmid.** 1981. Biochemical and immunological identification of cytokeratin proteins present in hepatocytes of mammalian liver tissue. Exp. Cell Res. **131**:299–318.
17. **Franke, W. W., H. Denk, E. Schmid, M. Osborn, and K. Weber.** 1979. Ultrastructural, biochemical, and immunologic characterization of Mallory bodies in livers of griseofulvin-treated mice: fimbriated rods of filaments containing prekeratin-like polypeptides. Lab. Invest. **40**:207–220.
18. **Franke, W. W., D. L. Schiller, R. Moll, S. Winter, E. Schmid, and I. Engelbrecht.** 1981. Diversity of cytokeratins. J. Mol. Biol. **153**:933–959.
19. **Franke, W. W., E. Schmid, and C. Grund.** 1982. Intermediate filament proteins in nonfilamentous structures: transient disintegration and inclusion of subunit proteins in granular aggregates. Cell **30**:103–113.
20. **Geisler, N., and K. Weber.** 1981. Self-assembly in vitro of the 68,000 molecular weight component of the mammalian neurofilament triplet proteins into intermediate-sized filaments. J. Mol. Biol. **151**:565–571.
21. **Geisler, N., and K. Weber.** 1981. Comparison of the proteins of two immunologically distinct intermediate-sized filaments by amino acid sequence analysis: desmin and vimentin. Proc. Natl. Acad. Sci. USA **78**:4120–4123.
22. **Gigi, O. B., B. Geiger, Z. Eshhar, R. Moll, E. Schmid, S. Winter, D. L. Schiller, and W. W. Franke.** 1982. Detection of a cytokeratin determinant common to diverse epithelial cells by a broadly cross-reacting monoclonal antibody. EMBO J. **1**:1429–1437.
23. **Giudice, G. J., and E. Fuchs.** 1987. The transfection of epidermal keratin genes into fibroblasts and simple epithelial cells: evidence for inducing a type I keratin by a type II gene. Cell **48**:453–463.
24. **Gronostajski, R. M., A. L. Goldberg, and A. B. Pardee.** 1984. Energy requirement for degradation of tumor-associated protein p53. Mol. Cell. Biol. **4**:442–448.
25. **Gunning, P., J. Leavitt, G. Muscat, S. Ng, and L. Kedes.** 1987. A human beta-actin expression vector system directs high-level accumulation of antisense transcripts. Proc. Natl. Acad. Sci. USA **84**:4831–4835.
26. **Hatzfeld, M., and W. W. Franke.** 1985. Pair formation and promiscuity of cytokeratins: formation in vitro of heterotypic complexes and intermediate-sized filaments by homologous and heterologous recombinations of purified polypeptides. J. Cell Biol. **101**:1826–1841.
27. **Herskowitz, I.** 1987. Functional inactivation of genes by dominant negative mutations. Nature (London) **329**:219–222.
28. **Howe, W. E., F. G. Klier, and R. G. Oshima.** 1986. Murine endodermal cytokeratins Endo A and Endo B are localized in the same intermediate filament. J Histochem. Cytochemistry **34**:785–793.
29. **Ichinose, Y., Z. Fengyun, S. Srimahasongcram, M. L. C. Tondella, M. Matsumoto, M. Nozaki, and A. Matsushiro.** 1988. Nucleotide sequence and structure of the mouse cytokeratin Endo B gene. Gene **70**:85–95.
30. **Klymkowsky, M. W., R. H. Miller, and E. B. Lane.** 1983. Morphology, behavior, and interaction of cultured epithelial cells after the antibody-induced disruption of keratin filament organization. J. Cell Biol. **96**:494–509.
31. **Kulesh, D. A., and R. G. Oshima.** 1988. Cloning of the human keratin 18 gene and its expression in nonepithelial mouse cells.

Mol. Cell. Biol. **8**:1540–1550.

32. **Leube, R. E., F. X. Bosch, V. Romano, R. Zimbelmann, H. Hofler, and W. W. Franke.** 1986. Cytokeratin expression in simple epithelia. III. Detection of mRNAs encoding human cytokeratins nos. 8 and 18 in normal and tumor cells by hybridization with cDNA sequences in vitro and in situ. Differentiation **33**:69–85.
33. **Liem, R. K. H., and S. B. Hutchison.** 1982. Purification of individual components of the neurofilament triplet: filament assembly from the 70000-dalton subunit. Biochemistry **21**:3221–3226.
34. **Magin, T. M., M. Hatzfeld, and W. W. Franke.** 1987. Analysis of cytokeratin domains by cloning and expression of intact and deleted polypeptides in Escherichia coli. EMBO J. **6**:2607–2615.
35. **Millan, J. L.** 1986. Molecular cloning and sequence analysis of human placental alkaline phosphatase. J. Biol. Chem. **261**: 3112–3115.
36. **Mizusawa, S., S. Nishimura, and F. Seela.** 1986. Improvement of the dideoxy chain termination method of DNA sequencing by use of deoxy-7-deazaguanosine triphosphate in place of dGTP. Nucleic Acids Res. **14**:1319–1324.
37. **Moll, R., W. W. Franke, D. L. Schiller, B. Geiger, and R. Krepler.** 1982. The catalog of human cytokeratins: patterns of expression in normal epithelia, tumors and cultured cells. Cell **31**:11–24.
38. **Moon, H. M., T. Wisniewski, P. Merz, J. De Martin, and H. M. Wisniewski.** 1981. Partial purification of neurofilament subunits from bovine brains and studies on neurofilament assembly. J. Cell Biol. **89**:560–567.
39. **Mulligan, R. C., and P. Berg.** 1981. Selection for animal cells that express the Escherichia coli gene coding for xanthine-guanine phosphoribosyltransferase. Proc. Natl. Acad. Sci. USA **78**:2072–2076.
40. **Oshima, R. G.** 1981. Identification and immunoprecipitation of cytoskeletal proteins from murine extra-embryonic endodermal cells. J. Biol. Chem. **256**:8124–8133.
41. **Oshima, R. G.** 1982. Developmental expression of murine extraembryonic endodermal cytoskeletal proteins. J. Biol. Chem. **257**:3414–3421.
42. **Oshima, R. G., W. E. Howe, F. G. Klier, E. D. Adamson, and L. H. Shevinsky.** 1983. Intermediate filament protein synthesis in preimplantation murine embryos. Dev. Biol. **99**:447–455.
43. **Oshima, R. G., J. L. Millan, and G. Cecena.** 1986. Comparison of mouse and human keratin 18: a component of intermediate filaments expressed prior to implantation. Differentiation **33**: 61–68.
44. **Oshima, R. G., K. Trevor, L. H. Shevinsky, O. A. Ryder, and G. Cecena.** 1988. Identification of the gene coding for the Endo B murine cytokeratin and its methylated, stable inactive state in mouse nonepithelial cells. Genes Dev. **2**:505–516.
45. **Quinlan, R. A., J. A. Cohlberg, D. L. Schiller, M. Hatzfeld, and W. W. Franke.** 1984. Hetertypic tetramer (A2D2) complexes of non-epidermal keratins isolated from cytoskeletons of rat hepatocytes and hepatoma cells. J. Mol. Biol. **178**:365–388.
46. **Quinlan, R. A., and W. W. Franke.** 1982. Heteropolymer filaments of vimentin and desmin in vascular smooth muscle tissue and cultured baby hamster kidney cells demonstrated by chemical crosslinking. Proc. Natl. Acad. Sci. USA **79**:3452–3456.
47. **Quinlan, R. A., and W. W. Franke.** 1983. Molecular interaction in intermediate-sized filaments revealed by chemical cross-linking. Eur. J. Biochem. **132**:477–484.
48. **Rogers, S., R. Wells, and M. Rechsteiner.** 1986. Amino acid sequences common to rapidly degraded proteins: the PEST hypothesis. Science **234**:364–368.
49. **Sanger, F., S. Nicklen, and A. R. Coulson.** 1977. DNA sequencing with chain-terminating inhibitors. Proc. Natl. Acad. Sci. USA **74**:5463–5467.
50. **Semat, A., M. Vasseur, L. Maillet, P. Brulet, and Y. M. Darmon.** 1988. Sequence analysis of murine cytokeratin Endo A (n°8) cDNA. Evidence for mRNA species initiated upstream of the normal 5′ end in PCC4 cells. Differentiation **37**:40–46.
51. **Singer, P. A., K. Trevor, and R. G. Oshima.** 1986. Molecular cloning and characterization of the Endo B cytokeratin expressed in preimplantation mouse embryos. J. Biol. Chem. **261**:538–547.
52. **Steinert, P. M., W. W. Idler, F. Cabral, M. M. Gottesman, and R. D. Goldman.** 1981. In vitro assembly of homopolymer and copolymer filaments from intermediate filament subunits of muscle and fibroblastic cells. Proc. Natl. Acad. Sci. USA **78**:3692–3696.
53. **Steinert, P. M., W. W. Idler, and S. B. Zimmerman.** 1976. Self-assembly of bovine keratin filaments in vitro. J. Mol. Biol. **108**:547–567.
54. **Steinert, P. M., and D. A. D. Parry.** 1985. Intermediate filaments: conformity and diversity of expression and structure. Annu. Rev. Cell Biol. **1**:41–65.
55. **Steinert, P. M., and D. R. Roop.** 1988. Molecular and cellular biology of intermediate filaments. Annu. Rev. Biochem. **57**: 593–625.

55a. **Sun, T.-T., R. Eichner, A. Schermer, D. Cooper, W. G. Nelson, and R. A. Weiss.** 1984. Classification, expression and possible mechanisms of evolution of mammalian epithelial keratins: a unifying model, p. 169–176. *In* A. Levine, W. Topp, G. Vande Woude and J. D. Watson (ed.), Cancer cells. I. The transformed phenotype. Cold Spring Harbor Laboratory, Cold Spring Harbor, N.Y.

56. **Vasseur, M., P. Duprey, P. Brulet, and F. Jacob.** 1985. One gene and one pseudogene for the cytokeratin Endo A. Proc. Natl. Acad. Sci. USA **82**:1155–1159.